

## Generation of transverse fluid currents and forces by an electric field: Electro-osmosis on charge-modulated and undulated surfaces

Armand Ajdari\*

*Lyman Laboratory, Physics Department, Harvard University, Cambridge, Massachusetts 02138*

(Received 5 September 1995)

As in the usual paradigm for electro-osmosis, an electrolyte fluid confined between two parallel plates is considered, and an electric field  $\vec{E}_{\text{ext}}$  is applied parallel to the plates. Analyzing here the combined effect of charge and shape modulation on the surfaces,  $E_{\text{ext}}$  is shown to generate flows in the slab and forces on the plates even if the plates (and thus the fluid) are on average neutral. Furthermore, the corresponding fluid current and plate drag are generically nonparallel to the field, and can be strictly perpendicular to it in well-chosen geometries.

PACS number(s): 82.65.Fr, 82.45.+z, 47.65.+a

### I. INTRODUCTION

An external electric field induces motion of an electrolyte fluid in the vicinity of a charged surface. The resulting relative velocity between the surface and fluid away from the surface leads to the well-known phenomena of electrophoresis and electro-osmosis [1–3]. Electrophoresis describes how a particle is set into motion when submitted to an electric field in a fluid at rest, and how its corresponding electrophoretic mobility depends on its surface characteristics: surface potential (“zeta” potential) or charge density [1–3]. Electro-osmosis describes the way immobile charged walls induce flow of the fluid they bound. Both are of great importance in separation technologies using electric fields, e.g., in the developing domain of capillary electrophoresis [4]. More recently, electro-osmosis has also been proposed as a self-propulsion mechanism for cells without motile apparatus: these are able to generate electric potential gradients, and, as their membrane is charged, motion is expected [3,5].

In this paper we investigate some features of the electro-osmotic flows generated on surfaces with nonuniform surface potentials (or charge densities). As such, this parallels the recent studies of Anderson and co-workers [3,6], who investigated the influence of such inhomogeneities on the electrophoretic mobility of small particles. The present analysis also displays features similar to those arising when an electric field induces charges at a fluid interface, which under the influence of the former in turn induce motion of the fluid [7]. The geometries we consider are also inspired by biophysical models for the flagellar rotatory motor of bacteria. In this system an ion flux across the membrane induces the rotation of a rotor (attached to the flagella) relative to a stator (attached to the cell body). The rotation axis is perpendicular to the membrane and thus parallel to the ionic current. Recent biophysical models picture the rotor as a cylinder coated by helical stripes of charges of opposite signs [8]. It is then tempting to investigate the possibility of mimicking

such geometries and effects in artificial devices at the micron scale [9]. More generally, with the increasing possibilities offered by lithographic techniques, electrohydrodynamic effects on striped patterns should be a developing field.

As a first step, the simple geometry of an electrolyte confined between two essentially planar insulating walls is considered. We investigate the effects of applying an electric field (actually an ionic current) parallel to the fluid channel. In Sec. II we introduce the notations and formalism used to describe the coupling between electrostatics and hydrodynamics, allowing us to recall in passing the well-known electro-osmotic effect: if the two walls are flat and uniformly charged, an applied electric field generates a plug flow in the slab. In Sec. III charge modulations on flat surfaces are shown to lead to convective patterns, but to be unable to generate net currents in the slab or forces on the walls. However, the combination of charge and shape modulation on the walls creates such currents and forces, even when the average charge on the walls (or in the electrolyte) is zero, and with components perpendicular to the applied field. Two geometries are explicitly considered: a neutral undulated plate on top of a flat charge-modulated one (Sec. IV), and a flat neutral plate on top an undulated charge-modulated one (Sec. V). A discussion (Sec. VI) concludes the paper. A preliminary report of some of the results was given in Ref. [10].

### II. ELECTROHYDRODYNAMIC COUPLING: EQUATIONS AND MODEL

Consider two almost flat parallel surfaces confining an electrolyte solution. The upper and lower surfaces are defined by  $z^+(x,y)$  and  $z^-(x,y)$  in a  $(x,y,z)$  system of Cartesian coordinates, with averages  $\langle z^+ \rangle = h$  and  $\langle z^- \rangle = -h$ . The electrolyte is of dielectric constant  $\epsilon$  and viscosity  $\eta$ , and its ionic content such that the Debye-Huckel length is  $\kappa^{-1}$ . The fluid is assumed to be incompressible, and a low Reynolds number description is valid.

The two bounding walls acquire a charge in contact with the electrolyte so that they bear a surface charge density  $\sigma^+(x,y)$  and  $\sigma^-(x,y)$ . Correspondingly, electroneutrality is violated in the fluid in their vicinity (Debye layer) [1]. The net charge density  $\rho_e^{\text{eq}}$  is related to the potential  $\psi^{\text{eq}}$  by the Poisson equation  $\epsilon \Delta \psi^{\text{eq}} + \rho_e^{\text{eq}} = 0$ . The potential on the sur-

\*On leave from Laboratoire de Physico-Chimie Théorique, ESPCI, 10 rue Vauquelin, 75231 Paris cedex 05, France, where correspondence should be addressed.

faces, often referred to as the ‘‘zeta’’ potential, is  $\zeta^\pm(x, y) = \psi^{\text{eq}}[x, y, z^\pm(x, y)]$ . The relation between zeta potentials and surface charge densities can be obtained from the Gouy-Chapman theory or from the Debye-Huckel linearized version if the potentials are small compared to thermal energies:  $e\zeta/k_B T \ll 1$  [1–3].

If an uniform external electric field  $\vec{E}_{\text{ext}}$  (or an electric current) is applied parallel to the slab, the nonzero charge density will drag the fluid in the  $\kappa^{-1}$ -thick Debye layer, inducing a nonzero velocity field  $\vec{v}$  everywhere in the slab. The coupling is described by a force density term in the Stokes equation:

$$\begin{aligned} -\vec{\nabla} p + \eta \Delta \vec{v} + \rho_e \vec{E} &= \vec{0}, \\ \vec{\nabla} \cdot \vec{v} &= 0, \end{aligned} \quad (1)$$

where  $\rho_e$  and  $\vec{E} = -\vec{\nabla} \psi$  are the total local charge densities and electric field (i.e., when  $\vec{E}_{\text{ext}}$  is applied), and  $p$  is the hydrodynamic pressure. This is in general a formidable problem as the bulk force term is nonlinear and in that the hydrodynamics furthermore influence the solution of the electrostatics problem through convective terms in the expression of ionic currents [2,3]. It is thus classically tractable only in the framework of linear response to the applied field  $\vec{E}_{\text{ext}}$  and through further approximations. We will here use two common examples presented in the next subsections: low electrostatic potentials (LEP’s) and thin Debye layers (TDL’s).

This provides us with the set of equations used throughout the paper. Note that they allow the addition of any purely hydrodynamic solution respecting the no-slip boundary conditions. We therefore focus without loss of generality on the case where no global pressure gradient exists across the system. It is also clear that we have chosen to study only steady-state situations.

#### A. Low electrostatic surface potentials

For low electrostatic potentials (LEP’s)  $e\zeta/k_B T \ll 1$  (typically  $\zeta \ll 25$  mV), the equilibrium electrostatics are conveniently described by the Debye-Huckel equation

$$\begin{aligned} \Delta \psi^{\text{eq}} &= \kappa^2 \psi^{\text{eq}}, \\ \partial_n \psi^{\text{eq}}(z^\pm) &= -\sigma^\pm / \epsilon, \end{aligned} \quad (2)$$

where  $\partial_n$  describes the derivative along the normal to the wall pointing inwards toward the electrolyte. For low applied fields the hydrodynamics problem can then be shown [2] to be well approximated by

$$\begin{aligned} -\vec{\nabla} p' + \eta \Delta \vec{v} + \rho_e^{\text{eq}} \vec{E}_{\text{ext}}^* &= \vec{0}, \\ \vec{\nabla} \cdot \vec{v} &= 0, \end{aligned} \quad (3)$$

where  $p' = p - \epsilon \kappa^2 (\psi^{\text{eq}})^2 / 2 + (\rho_e - \rho_e^{\text{eq}}) \psi^{\text{eq}}$ , and  $\vec{E}_{\text{ext}}^*(\vec{r}) = -\vec{\nabla} V_{\text{ext}}^*$  is the electric field corresponding to an average field  $\vec{E}_{\text{ext}}$  imposed between insulating walls of the same shape in the vacuum (i.e., obtained by simple solution of the Laplace equation  $\Delta V_{\text{ext}}^* = 0$  with boundary conditions  $\partial_n V_{\text{ext}}^* = 0$  on the surfaces). Note that  $\vec{E}_{\text{ext}}^*$  was confusingly designed by  $\vec{E}_{\text{ext}}$  in Eqs. (2) and (3) of Ref. [10], where was taken into

account the fact that *for flat parallel walls*  $\rho_e - \rho_e^{\text{eq}}$  is negligible. The above formulation (3) is more general and adequate for nonplanar boundaries.

#### B. Thin Debye layers

If the Debye layers are very thin (TDL’s) compared to both the typical radii of curvature of the surfaces, the distance between surfaces, and the typical distance of variation of the charge densities [more precisely, smaller than these lengths by at least a factor  $\sim \exp(e\zeta/2k_B T)$  [3]], then in a linear response theory, it is possible to approximate the electrohydrodynamic problem (1) by the simple Stokes equation

$$\begin{aligned} -\vec{\nabla} p + \eta \Delta \vec{v} &= \vec{0}, \\ \vec{\nabla} \cdot \vec{v} &= 0 \end{aligned} \quad (4)$$

upon replacement of the (up to now implicit) no-slip boundary conditions on the surfaces by slip boundary conditions [3],

$$\vec{v}(x, y, z^\pm) = \mu^\pm(x, y) \vec{E}_{\text{ext}}^*(x, y, z^\pm), \quad (5)$$

with, from local analysis,

$$\mu(x, y) = -\epsilon \zeta^\pm(x, y) / \eta. \quad (6)$$

This great simplification, which is often valid as the Debye length in usual conditions (1-1 salt in water at  $10^{-1} - 10^{-3} M l^{-1}$ ) is  $\approx 1 - 10$  nm, allows the calculation of electrophoretic mobilities for various particle shapes, and to take into account variations of the surface potential [3,6]. Note that the TDL regime is not a subcase of the LEP approach, as it allows us to describe high electric potentials, in which the relation between the surface charge and zeta potential is incorrectly described by the Debye-Huckel approximation. The two approaches of course coincide in the case of low potentials *and* thin Debye layers. As a quick example we recall in Sec. III C the usual theory of electro-osmosis between uniformly charged flat plates, before turning to inhomogeneous surface charge distributions in Sec. III.

#### C. Electro-osmosis on homogeneous surfaces

Consider two flat surfaces  $z^\pm = \pm h$  with uniform charge distribution  $\sigma^+ = \sigma^- = \sigma_0$ . In the LEP regime the equilibrium electric potential inside the solution is, from (2),  $\psi^{\text{eq}}(z) = \zeta_0 \cosh(\kappa z) / \cosh(\kappa h)$ , where  $\zeta_0 = \sigma_0 \coth(\kappa h) / \epsilon \kappa$ . For flat plates one has simply  $\vec{E}_{\text{ext}}^* = \vec{E}_{\text{ext}}$  everywhere, so that (3) leads to  $\vec{v} = (\epsilon / \eta) [\psi^{\text{eq}}(z) - \zeta_0] \vec{E}_{\text{ext}}$ . For  $\kappa h \gg 1$ , apart from the Debye layers close to the walls, the velocity is thus almost uniform  $\vec{v} \approx \mu_0 \vec{E}_{\text{ext}}$  with  $\mu_0 = -\epsilon \zeta_0 / \eta$  (electro-osmotic plug flow). The minus sign is easily understood: if  $\zeta_0$  is positive, negative charges are in excess close to the surfaces, and the fluid there is driven in a direction opposite to that of  $\vec{E}_{\text{ext}}$ .

The LEP result is clearly consistent with the TDL approach, which leads simply to  $\vec{v} = \mu_0 \vec{E}_{\text{ext}}$  everywhere, omitting the description of the flow in the Debye layers. An electro-osmotic plug flow is created in the slab, which has to be taken into account, e.g., when analyzing capillary electrophoresis data [4].

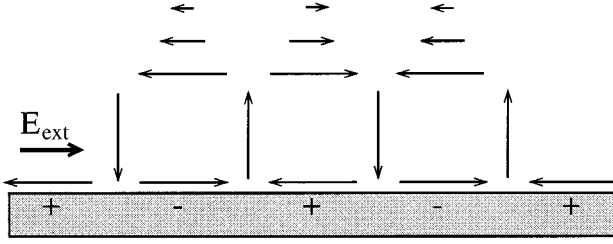


FIG. 1. Close to a charge-modulated surface, the fluid is pulled periodically in opposite directions. As a result, recirculation rolls develop on a scale proportional to the modulation wavelength.

### III. FLAT PLATES WITH MODULATED SURFACE CHARGES

Now consider inhomogeneously charged flat surfaces. Due to the linearity of the equations, solving the generic problem with arbitrary surface charge densities on the two surfaces reduces for each wave vector to the analysis of two geometries, which we choose, for formal simplicity, to provide even and odd solutions in  $z$ . In the first one the surfaces are charged in a symmetric way:  $\sigma_1^+(x) = \sigma_1^-(x) = \sigma_0 \cos(qx)$ . In the second one, the sign of the charge on the lower plate is reversed (or its phase shifted by  $\pi$ ):  $\sigma_2^+(x) = \sigma_0 \cos(qx)$  on the upper plate and  $\sigma_2^-(x) = -\sigma_0 \cos(qx)$  on the lower plate. In most of this section we adopt the formalism corresponding to the LEP limit, and on our way will mention the corresponding (and simpler) results for the TDL case.

Using the Debye-Huckel equation (2), the equilibrium electrostatic potentials in these two geometries are easily obtained. They read (omitting the “eq” to simplify notations)

$$\psi_1(x, z) = (\sigma_0 / Q\epsilon) \cos(qx) \frac{\cosh(Qz)}{\sinh(Qh)}, \quad (7)$$

$$\psi_2(x, z) = (\sigma_0 / Q\epsilon) \cos(qx) \frac{\sinh(Qz)}{\cosh(Qh)}, \quad (8)$$

with  $Q^2 = q^2 + \kappa^2$ . For flat plates one has uniformly  $\vec{E}_{\text{ext}}^* = \vec{E}_{\text{ext}}$ , which simplifies solving (3).

#### A. $\vec{E}_{\text{ext}}$ parallel to the modulation wave vector

If an external field is applied along this axis  $\vec{E}_{\text{ext}}^{\parallel} = E_{\parallel} \vec{x}$ , the fluid close to the surfaces is driven in a direction that alternates along the  $x$  axis. Incompressibility imposes recirculation in the slab, and convective rolls appear (Fig. 1). The velocity field is most easily derived by exploiting the incompressibility condition in (3) to introduce a stream function  $\phi(x, z)$  such that  $\partial_z \phi = v_x$  and  $\partial_x \phi = -v_z$ . In the two above-mentioned geometries some algebra allows us to obtain

$$\phi_i(x, z) = \mu_0 E_{\parallel} \cos(qx) g_i(z) \quad (9)$$

with  $\mu_0 = -\sigma_0 / \eta\kappa$ ,

$$g_1 = A[a_1 z \cosh(qz) + a_2 h \sinh(qz) + a_3 \sinh(Qz)], \quad (10)$$

$$A = [\kappa \sinh(Qh)]^{-1} [hq - \sinh(qh) \cosh(qh)]^{-1}, \quad (11)$$

$$a_1 = q \sinh(Qh) \cosh(qh) - Q \cosh(Qh) \sinh(qh), \quad (12)$$

$$a_2 = Q \cosh(Qh) \cosh(qh) - q \sinh(Qh) \sinh(qh) - h^{-1} \sinh(Qh) \cosh(qh), \quad (13)$$

$$a_3 = \sinh(qh) \cosh(qh) - hq \quad (14)$$

and

$$g_2 = B[b_1 z \sinh(qz) + b_2 h \cosh(qz) + b_3 \cosh(Qz)], \quad (15)$$

$$B = -[\kappa \cosh(Qh)]^{-1} [hq + \sinh(qh) \cosh(qh)]^{-1}, \quad (16)$$

$$b_1 = q \cosh(Qh) \sinh(qh) - Q \sinh(Qh) \cosh(qh), \quad (17)$$

$$b_2 = Q \sinh(Qh) \sinh(qh) - q \cosh(Qh) \cosh(qh) - h^{-1} \cosh(Qh) \sinh(qh), \quad (18)$$

$$b_3 = \sinh(qh) \cosh(qh) + hq. \quad (19)$$

Due to the linearity of the problem, these solutions determine the influence of each plate. That is, if only the upper plate is charged with  $\sigma_+ = \sigma_0 \cos(qx)$ , the resulting stream function is  $\phi_+ = (\phi_1 + \phi_2)/2$ . Similarly, if only the lower plate has the previous modulation,  $\phi_- = (\phi_1 - \phi_2)/2$ . Then, for any charge modulation of the surfaces, the linearity of the problem allows us, by Fourier decomposition, to sum the contribution of each wavelength on each plate.

Let us recall at this point that the iso- $\phi$  lines are the stream lines of the flow. Thus a contour plot of  $\phi$  is an easy way to visualize the convection pattern induced by  $\vec{E}_{\text{ext}}^{\parallel}$  [10]. The velocity field is more quantitatively described by

$$\begin{aligned} v_x &= \mu_0 E_{\parallel} \cos(qx) g'(z), \\ v_z &= \mu_0 E_{\parallel} \sin(qx) qg(z), \end{aligned} \quad (20)$$

where  $g$  is the linear combination of  $g_1$  and  $g_2$  appropriate to fit the given electrostatic boundary conditions. In the next two subsections we analyze the morphology of the convective patterns in a few geometries.

#### B. Single plate (the $hq \gg 1$ limit)

Take the bottom plate charged  $\sigma^- = \sigma_0 \cos(qx)$ , and the gap much larger than the modulation wavelength  $2\pi/q$  (and than the Debye length  $\kappa^{-1}$ ). Focusing on the vicinity of the lower plate  $z_> = z + h \ll h$ , the influence of the upper plate is negligible. Thus from direct calculation or using the results of Sec. III A, the stream function for a parallel field is

$$\phi \approx \mu_0 E_{\parallel} \cos(qx) g(z_>), \quad (21)$$

where

$$g(z_>) = \kappa^{-1} \{ [(Q - q)z_> - 1] e^{-qz_>} + e^{-Qz_>} \}. \quad (22)$$

Recirculation of the flow induced in the Debye layers occurs on a scale given by the point at which  $g'(z_>)$  (and thus  $v_x$ ) changes sign (Fig. 1). This occurs at a distance  $\delta$  from the wall such that

$$[(Q-q)(1-q\delta)+q]e^{-q\delta}-Qe^{-Q\delta}=0. \quad (23)$$

For  $\kappa \gg q$  this leads to  $q\delta \approx 1$ . At distances larger than  $\delta$  the flow along  $x$  is in the direction opposite to what it is close to the surface, and decays exponentially on the same scale  $\delta$ .

### C. Narrowing the gap

Starting from the previous one-plate description, let us progressively narrow the gap in the face-to-face geometry 1 described by Eq. (7) when a parallel field is applied. When the two surfaces are far apart, they develop almost noninteracting patterns, the exponential tails in the stream function melting in a cosh shape. A plot of  $v_x(z)$  thus displays five local extrema: the electro-osmotic flows peak close to the walls, and the recirculating flows peak at a distance of order  $\delta$  and decrease until the middle of the slab  $z=0$  which is a local minima. If the plates are brought closer, the two patterns tend to ‘‘compress’’ each other, and the  $z$  size of the rolls becomes  $h$ . In this geometry, the recirculating flows of the two surfaces merge in the middle of the slab so that  $v_x(z)$  only has three extrema, recirculation peaking at  $z=0$ . The transition occurs for  $\partial_z^3 g_1(0)=0$ . Although the corresponding equation is cumbersome, namely  $3q^2 a_1 + hq^3 a_2 + Q^3 a_3 = 0$ , it reduces in the limit of a thin Debye layer ( $\kappa \gg q, h^{-1}$ ) to the much simpler  $\tanh(qh) = qh/3$ , or  $qh = 2.98 \approx 3$ . Note that in the limit  $\kappa \gg h^{-1} \gg q$ , the flow is easily shown to be locally (at a given  $x$ ) the sum of a simple pluglike electro-osmotic flow corresponding to the local value  $\sigma(x)$  and of a Poiseuille recirculation flow due to local gradients of the pressure (recall that no large scale pressure gradient is allowed), so that there is no net current:

$$v_x \approx \mu_0 E_{\parallel} \cos(qx) \left[ 1 - e^{\kappa(z-h)} - e^{-\kappa(z+h)} - \frac{3}{2} \frac{(h^2 - z^2)}{h^2} \right]. \quad (24)$$

An even clearer transition is obtained when the potential modulations of the two surfaces are identical but for a phase shift of  $\pi$  (geometry 2). Then again, when  $h \gg q^{-1}$ , the two surfaces develop almost independent convective patterns. But upon narrowing of the gap, the system chooses to rearrange them so as to reduce dissipation due to shear: recirculation now brings the fluid directly from one surface to the other along a given streamline. The transition is clear on a plot of  $v_x(z)$  which displays four local extrema for  $qh \gg 1$  and only two for  $qh \ll 1$ . The critical value is given by  $\partial_z^2 g_2(0)=0$  or  $2qb_1 + hq^2 b_2 + Q^2 b_3 = 0$ . For a thin Debye layer, this leads to  $\coth(qh) = qh/2$ , or  $qh = 2.07 \approx 2$ .

Patterns corresponding to phase shifts of the modulation intermediate between 0 and  $\pi$ , or modulations of different amplitudes or wavelengths on the two plates, are easily computed from Eq. (20).

### D. $\vec{E}_{\text{ext}}$ perpendicular to the modulation wave vector

If an external field  $\vec{E}_{\text{ext}}^{\perp}$  is applied perpendicularly to the potential modulation  $\vec{E}_{\text{ext}}^{\perp} = E_{\perp} \vec{y} = \vec{E}_{\text{ext}}^*$  the equations are much easier to solve as only  $v_y(x, z)$  is nonzero. Actually (3) requires that  $v_y - \epsilon E_{\perp} \psi / \eta$  be a harmonic function. Imposing  $v_y = 0$  on the plates then leads in the two previous electrical geometries to

$$\vec{v}_1 = -\frac{\sigma_0 \vec{E}_{\text{ext}}^{\perp}}{\eta Q} \coth(Qh) \cos(qx) \left[ \frac{\cosh(qz)}{\cosh(qh)} - \frac{\cosh(Qz)}{\cosh(Qh)} \right], \quad (25)$$

$$\vec{v}_2 = -\frac{\sigma_0 \vec{E}_{\text{ext}}^{\perp}}{\eta Q} \tanh(Qh) \cos(qx) \left[ \frac{\sinh(qz)}{\sinh(qh)} - \frac{\sinh(Qz)}{\sinh(Qh)} \right]. \quad (26)$$

Close to each plate, the electric field drives the fluid along  $y$  with a sign that alternates along  $x$ . This surface effect tends to disappear (and the velocity to reach its average value zero) over a distance  $\approx q^{-1}$  in the  $z$  direction. So if  $qh \gg 1$  the two plates develop almost independent periodic shear flows, whereas they interact if  $qh \ll 1$ .

### E. Thin Debye layer limit: $\kappa \gg q, h$

If the Debye length is much thinner than both the slab gap  $h$  and the wavelength of the charge modulation  $2\pi/q$ , Eq. (9) for a parallel field is valid for (10 and 15) simplified along

$$g_1(z) \approx \frac{h \cosh(qh) \sinh(qz) - z \sinh(qh) \cosh(qz)}{hq - \sinh(qh) \cosh(qh)}, \quad (27)$$

$$g_2(z) \approx \frac{z \cosh(qh) \sinh(qz) - h \sinh(qh) \cosh(qz)}{hq + \sinh(qh) \cosh(qh)}. \quad (28)$$

For a perpendicular field, (21) and (22) give

$$\vec{v}_1 \approx \mu_0 \cos(qx) \vec{E}_{\text{ext}}^{\perp} \left[ \frac{\cosh(qz)}{\cosh(qh)} \right], \quad (29)$$

$$\vec{v}_2 \approx \mu_0 \cos(qx) \vec{E}_{\text{ext}}^{\perp} \left[ \frac{\sinh(qz)}{\sinh(qh)} \right]. \quad (30)$$

Formulas (27)–(30) are in fact obtained from scratch in the TDL approach for surface potentials  $\zeta_1^{\pm} = \zeta_0 \cos(qx)$  and  $\zeta_2^{\pm} = \pm \zeta_0 \cos(qx)$  using the slip boundary conditions (5) and (6) and  $\mu_0 = -\epsilon \zeta_0 / \eta$ . From (7) and (8) the two expressions for  $\mu_0$  indeed coincide in the combined LEP and TDL limits.

### F. Symmetry argument: Absence of net flow or force

In the geometries considered above, modulations of the charge densities at any finite wavelength produce a periodic flow pattern. As such they are unable to induce a *net* fluid current in the slab. Neither do they generate a net force on the plates. Therefore, only the  $q=0$  component of the surface charge density is important regarding these net (aver-

age) effects. This is clearly due to the symmetry between  $+$  and  $-$  charges that react in an exactly opposite way in an applied field.

To generate net effects in modulated geometries it is thus necessary to break this symmetry. A simple way to do so is to make the gap narrower at the location of charges of a given sign. Consider, e.g., a charge-modulated bottom wall  $\sigma^- = \sigma_0 \cos(qx)$ . Then an applied parallel field  $\vec{E}_{\text{ext}}^{\parallel}$  tends to push the fluid upwards for  $qx = -\pi/2$  modulo  $2\pi$ , and pull it downwards for  $qx = \pi/2$  modulo  $2\pi$ . By adding an upper undulated neutral surface  $z^+ = h[1 + \alpha \cos(qx)]$ , with  $\alpha > 0$  (see Fig. 2), the upward stream is ‘bent’ to the right (direction of  $\vec{E}_{\text{ext}}^{\parallel}$ ), whereas the downward stream pumps liquid from the left. It is thus natural to expect an *average current* to the right. We quantify this statement in Sec. IV. To describe in the clearest way the generation of these net effects, the formally simpler TDL limit is adopted in the rest of this paper.

#### IV. UNDULATED PLATE ON TOP OF A CHARGE-MODULATED SURFACE

Consider more generally a neutral undulated plate  $z^+ = h[1 + \alpha \cos(qx + \Phi)]$  on top of a flat one  $z^- = -h$ . The potential on the bottom one is modulated  $\zeta^- = \zeta_0 \cos(qx)$ . In the TBL limit, we use  $\mu_0 = -\epsilon \zeta_0 / \eta$  and thus have to solve a Stokes problem with boundary conditions  $\vec{v}(x, -h) = \mu_0 \cos(qx) \vec{E}_{\text{ext}}^*(x, -h)$  on the lower plate, and  $\vec{v}(z^+) = \vec{0}$  on the upper one. To allow analytical treatment, we furthermore consider small values of  $\alpha$  and thus take a perturbative approach:

$$\vec{v} = \vec{v}^{(0)} + \alpha \vec{v}^{(1)} + \dots, \quad (31)$$

$$\vec{E}_{\text{ext}}^* = \vec{E}_{\text{ext}}^{*(0)} + \alpha \vec{E}_{\text{ext}}^{*(1)} + \dots. \quad (32)$$

The inhomogeneity of the field  $\vec{E}_{\text{ext}}^*$  is a feature that actually appears in the case of a parallel applied field, which we address in Sec. IV A. We seek the generation of net fluid current and force on the upper plate at first order in  $\alpha$ , as the  $+$ – $-$  symmetry is readily broken at this order.

##### A. $\vec{E}_{\text{ext}}$ parallel to charge modulation and undulation

We first compute the field  $\vec{E}_{\text{ext}}^*$  corresponding to an applied (average) parallel field  $\vec{E}_{\text{ext}}^{\parallel} = E_{\parallel} \vec{x}$ . The zeroth order  $\vec{E}_{\text{ext}}^{*(0)} = \vec{E}_{\text{ext}}^{\parallel}$  (solution for flat plates) is used to solve the Laplace equation with field tangent to the surfaces at first order. This leads to the quantity of interest

$$\vec{E}_{\text{ext}}^{*(1)}(x, -h) = -\frac{qh}{\sinh(2qh)} \cos(qx + \Phi) \vec{E}_{\text{ext}}^{\parallel}. \quad (33)$$

Note that this adds a new element to the qualitative discussion given in Sec. III F: the electric field is stronger in the regions where the gap is narrower. The charges at these locations will therefore be more efficient in dragging the fluid. This additional effect is clearly seen from Fig. 2 to be in the same direction as the one previously mentioned in Sec. III F.

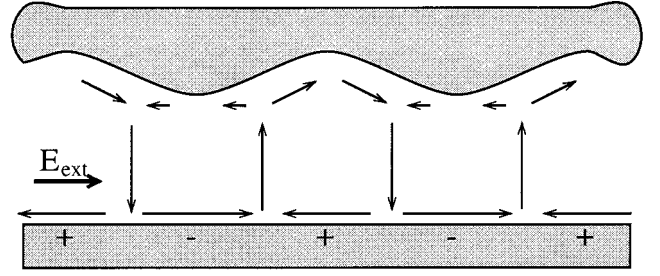


FIG. 2. An undulated surface on top of a flat charge-modulated one. Parallel applied field. The recirculation pattern due to the charge modulation is bent by the undulation to produce a net flow toward the right. This effect is enhanced by the fact that the electric field is more intense in narrower regions, thus inducing a stronger electro-osmotic slip velocity (longer arrows).

The zeroth order velocity field  $\vec{v}^{(0)}$  for a flat upper plate is given by Eq. (20), using the approximate formulas (23) and (24), or

$$g(z) = \frac{hqz_{<} \sinh(qz_{>}) - \sinh(qh) \cosh(qh) z_{>} \sinh(qz_{<})}{2[\sinh^2(qh) \cosh^2(qh) - h^2 q^2]}, \quad (34)$$

where  $z_{<} = z - h$  and  $z_{>} = z + h$ .

The zero velocity boundary condition on the upper plate  $\vec{v}(z^+) = \vec{0}$  leads at first order in  $\alpha$  to

$$\vec{v}^{(1)}(h) = -h \cos(qx + \Phi) \partial_z \vec{v}^{(0)}(h). \quad (35)$$

Noting, furthermore, that  $v_x^{(0)}(h) = 0$  implies  $g'(h) = 0$ , one is led to

$$\begin{aligned} v_x^{(1)}(h) &= -\mu_0 E_{\parallel} h g''(h) \cos(qx) \cos(qx + \Phi), \\ v_z^{(1)}(h) &= 0. \end{aligned} \quad (36)$$

The boundary condition on the lower plate is  $\vec{v}^{(1)}(-h) = \mu_0 \cos(qx) \vec{E}_{\text{ext}}^{*(1)}(-h)$ . Thus, as  $\cos(qx) \cos(qx + \Phi) = \cos(\Phi)/2 + \cos(2qx + \Phi)/2$ , one can decompose  $\vec{v}^{(1)} = \vec{u} + \vec{w}$ , where  $\vec{u}$  derives from a stream function proportional to  $\cos(2qx + \Phi)$  and can be calculated using formulas similar to (23) and (24), and  $\vec{w}$  is a simple shear flow,

$$\vec{w} = -\frac{\mu_0 \vec{E}_{\text{ext}}^{\parallel} \cos(\Phi)}{2} \left[ h g''(h) \frac{z+h}{2h} - \frac{qh}{\sinh(2qh)} \frac{z-h}{2h} \right], \quad (37)$$

which clearly appears as the sum of the shear flows imposed by the constant terms in the boundary conditions on the top and bottom plates. Although  $\vec{u}$  is periodic in  $x$  and carries no net flow, the shear flow  $\vec{w}$  does. Thus a net average current  $\vec{J}_{\parallel}$  is generated in the slab:

$$\vec{J}_{\parallel} = \int_{z^-}^{z^+} v_x dz = -\frac{\mu_0 h}{2} \vec{E}_{\text{ext}}^{\parallel} \alpha \cos(\Phi) f_{\parallel}(qh), \quad (38)$$

with, from (37) and (34),

$$f_{\parallel}(u) = u \frac{\cosh(2u)[2u - \tanh(2u)]}{2[\sinh^2(u) \cosh^2(u) - u^2]} + \frac{u}{\sinh(2u)}. \quad (39)$$

Changing the sign of  $\alpha$  is (fortunately) seen to be identical to shifting  $\Phi$  by  $\pi$ . The rescaled susceptibility  $f_{\parallel}(u)$  is positive for all values of  $u = qh$ . Thus if  $\zeta_0 > 0$ ,  $\Phi = 0$ , and  $\alpha > 0$ , we obtain  $\vec{J}_{\parallel}$  in the same direction as  $\vec{E}_{\text{ext}}^{\parallel}$  (recall that  $\mu_0$  is then negative). This is in agreement with the qualitative picture sketched in Sec. III F. Note that actually the first term on the right-hand side of (39) corresponds to that picture, while the second one is due to the increase of field intensity in the narrower regions (33). Both operate in the same direction.

We have thus shown that in this geometry *where the average charge in the solution is zero*, it is indeed possible to generate a fluid current by applying an external field. To reverse the direction of the current one can simply reverse the field or move the upper plate by  $\pi/q$ . Formula (38), although obtained for small  $\alpha$ , clearly shows that the effect is stronger for small values of  $qh$ , as expected: the two plates influence each other more efficiently. Actually,  $f_{\parallel}(qh) \approx 8(qh)^2 \exp(-2qh)$  for large  $qh$  and  $f_{\parallel}(qh) \approx \frac{3}{2}$  for small  $qh$ .

The flow in this situation also generates a net average stress on the upper plate. Its horizontal part  $\vec{\tau}_{\parallel}$  is given by

$$\vec{\tau}_{\parallel} \cdot \vec{x} = \langle -\eta \vec{n} \cdot [\vec{\nabla} \vec{v} + {}^t(\vec{\nabla} \vec{v})] \cdot \vec{x} + p \vec{n} \cdot \vec{x} \rangle_{z=z^+}, \quad (40)$$

where  $\vec{n}$  is the upwards normal to the top surface: at zeroth order  $\vec{n}^{(0)} = \vec{z}$  and at first order  $\vec{n}^{(1)} = qh \sin(qx + \Phi) \vec{x}$ . Gathering the many terms that appear in (40), the net stress on the upper surface to first order in  $\alpha$  is

$$\vec{\tau}_{\parallel} = -\frac{\eta \mu_0 \vec{E}_{\text{ext}}^{\parallel}}{4h} \alpha \cos(\Phi) k_{\parallel}(qh), \quad (41)$$

where

$$k_{\parallel}(u) = -u \frac{\cosh(2u)[2u - \tanh(2u)]}{2[\sinh^2(u)\cosh^2(u) - u^2]} + \frac{u}{\sinh(2u)} \quad (42)$$

is a negative function for all values of  $u = qh$ . From  $\approx -\frac{1}{2}$  for small  $u$  it decays exponentially when the gap is increased beyond the wavelength. Note that, contrary to the current, there is no direct argument giving the sign of  $k_{\parallel}$  as the pressure terms and the viscous drag terms are of opposite signs. Note eventually that we have chosen a sign convention for  $k_{\parallel}$  different than in Ref. [10] for the sake of similarity between (38) and (41).

If the upper plate is allowed to move along  $x$ , its equilibrium position will correspond to no current situations  $\Phi = \pm \pi/2$ , one of them (modulo  $2\pi$ ) being stable while the other one is not.

### B. Perpendicular field $\vec{E}_{\text{ext}}^{\perp}$

If an electric field  $\vec{E}_{\text{ext}}^{\perp} = E_{\perp} \vec{y}$  is applied perpendicular to the modulation, the electrostatics problem is simpler as  $\vec{E}_{\text{ext}}^* = \vec{E}_{\text{ext}}^{\perp}$  uniformly. The hydrodynamic problem is easily solved as  $\vec{v} = v_y(x, z) \vec{y}$ . The zeroth-order velocity is

$$\vec{v}^{(0)} = -\mu_0 \vec{E}_{\text{ext}}^{\perp} \cos(qx) \frac{\sinh[q(z-h)]}{\sinh(2qh)}; \quad (43)$$

therefore the boundary conditions for the first-order term are  $\vec{v}^{(1)}(-h) = \vec{0}$ , and, from (35),

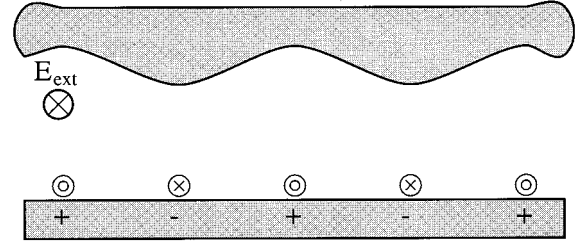


FIG. 3. An undulated surface on top of a flat charge-modulated one. Perpendicular applied field. Narrow regions are more efficient to induce stress on the upper plate but less efficient in contributing to the average current.

$$\vec{v}^{(1)}(h) = \mu_0 \vec{E}_{\text{ext}}^{\perp} \frac{hq}{2 \sinh(2qh)} [\cos \Phi + \cos(2qx + \Phi)]. \quad (44)$$

To this order, in addition to a periodic flow, we obtain a net shear flow and an average current

$$\vec{J}_{\perp} = -\frac{\mu_0 h}{2} \vec{E}_{\text{ext}}^{\perp} \alpha \cos(\Phi) f_{\perp}(qh), \quad (45)$$

with

$$f_{\perp}(u) = -\frac{u}{\sinh(2u)} < 0. \quad (46)$$

A net stress on the upper plate is also generated, which from a formula similar to (40) is

$$\vec{\tau}_{\perp} = -\frac{\eta \mu_0 \vec{E}_{\text{ext}}^{\perp}}{4h} \alpha \cos(\Phi) k_{\perp}(qh), \quad (47)$$

where

$$k_{\perp}(qh) = -f_{\perp}(qh) = \frac{qh}{\sinh(2qh)} > 0. \quad (48)$$

Formulas (45) and (47) respect the symmetries of the problem, and one can check the signs through the simple following physical argument, valid for small  $qh$ . Take  $\zeta_0 > 0$ ,  $\alpha > 0$ , and  $\Phi = 0$ . Then the slab is narrower in the regions where the charge density in the solution is positive (Fig. 3). The local current is the average velocity *times* the local thickness of the slab. The average velocity is roughly half that of the slip boundary condition, and is thus in modulus similar for negative and positive charge regions. The local current is thus stronger in the regions of negative charge densities, which leads to an overall current in the direction opposite to  $\vec{E}_{\text{ext}}$ . On the other hand, the viscous stress on the upper plate is the slip velocity times the viscosity *divided* by the slab thickness. Thus the narrower regions determine the sign of the drag, along  $\vec{E}_{\text{ext}}$  in the present case. As  $\mu_0 < 0$ , this is in agreement with (45).

Clearly for large values of  $qh$ ,  $f_{\perp}$  and  $k_{\perp}$  both decay exponentially as the charge and shape modulations do not interact, which they do for small  $qh$ , when  $f_{\perp}(qh) = -k_{\perp}(qh) \approx -\frac{1}{2}$ .

The pumping effect and drag force are thus of similar amplitude, although of opposite direction, if the electric field

is applied perpendicular or parallel to the modulations. This allows generation of fluid currents or forces purely transverse to the applied field  $\vec{E}_{\text{ext}}$ , as will be discussed in subsection IV D. Before that, a partial but simple check for the cumbersome calculations of the past two subsections is presented. More precisely, I focus on the  $qh \ll 1$  limit using the lubrication approximation.

### C. Lubrication approximation $qh \ll 1$

Consider a narrow channel of arbitrary local thickness  $d(x)$  above a flat surface at  $z_>=0$ . The bottom flat surface bears a modulated potential  $\zeta(x)$ . Variations along  $x$  of all quantities occur on scales larger than the typical channel thickness.

Let us first apply an electric current  $J_{\text{el}}^{\parallel}$  along  $x$  in this channel (parallel geometry). This imposes a local electric field  $E(x)$  (neglecting in this limit variations along  $z_>$ ) given by the conservation of the electric current:  $J_{\text{el}}^{\parallel} = cE(x)d(x)$ , where  $c$  is the conductivity of the electrolyte. This field acting on the lower boundary imposes a shear current  $\mu(x)E(x)d(x)/2$ , with  $\mu(x) = -\epsilon\zeta(x)/\eta$ . Taking into account the Poiseuille flow generated by local pressure gradients along  $x$  the conservation of the total fluid current  $J_{\parallel}$  reads

$$J_{\parallel} = \frac{1}{2}\mu(x)E(x)d(x) - \frac{1}{12\eta} \partial_x p(x)d^3(x). \quad (49)$$

This allows us to calculate pressure differences as a function of the constants  $J_{\text{el}}^{\parallel}$  and  $J_{\parallel}$ , and of the shape  $d(x)$ . Insisting that we have no buildup of pressure across the system  $\langle \partial_x p \rangle = 0$  gives the fluid current as a function of the electrical current,

$$J_{\parallel} = \frac{J_{\text{el}}^{\parallel}}{2c} \frac{\langle \mu(x)/d^3(x) \rangle}{\langle 1/d^3(x) \rangle}, \quad (50)$$

where  $\langle \rangle$  indicates the average in the  $x$  direction. Applying this general formula to our previous charge and shape modulations  $\zeta(x) = \zeta_0 \cos(qx)$  and  $d(x) = 2h[1 + \alpha \cos(qx + \Phi)/2]$ , with  $J_{\text{el}}^{\parallel} = 2hcE_{\parallel}$  to first order in  $\alpha$ , one recovers (38) with  $f_{\parallel} = \frac{3}{2}$ , which is the limit we found for  $qh \ll 1$ . Similar calculations, taking carefully into account both viscous shear and pressure effects, allow us to recover the corresponding values for  $\vec{\tau}$ .

For the case of a perpendicular field (or electric current), due to translational invariance, the absence of macroscopic pressure gradients impose that of local pressure gradients, so that the current is only due to the shear term

$$J_{\perp} = \frac{E_{\perp}}{2} \langle \mu(x)d(x) \rangle. \quad (51)$$

Similarly  $\mu$  simply has

$$\tau_{\perp} = \eta E_{\perp} \langle \mu(x)/d(x) \rangle. \quad (52)$$

When applied to the geometry considered in Sec. IV B, these two formulas agree with (45) and (47) and  $f_{\perp} = -k_{\perp} = -\frac{1}{2}$ , and quantify the qualitative argument given there.

### D. Generic field $\vec{E}_{\text{ext}} = E_{\parallel}\vec{x} + E_{\perp}\vec{y}$ and discussion

Now consider a generic applied field applied at an angle  $\theta$  with the direction  $x$ :  $\vec{E}_{\text{ext}} = E_{\parallel}\vec{x} + E_{\perp}\vec{y} = E_{\text{ext}}\vec{u}_{\theta}$ , where  $\vec{u}_{\theta} = \cos\theta\vec{x} + \sin\theta\vec{y}$ . Then the net fluid current and force on the upper plate are, to first order in  $\alpha$ ,

$$\vec{J}_{\parallel} = -\frac{\mu_0 h E_{\text{ext}}}{2} \alpha \cos(\Phi) \vec{f}(qh, \theta), \quad (53)$$

$$\vec{\tau}_{\parallel} = -\frac{\eta \mu_0 E_{\text{ext}}}{4h} \alpha \cos(\Phi) \vec{k}(qh, \theta), \quad (54)$$

where

$$\vec{f}(qh, \theta) = f_{\parallel}(qh) \cos\theta \vec{x} + f_{\perp}(qh) \sin\theta \vec{y}, \quad (55)$$

$$\vec{k}(qh, \theta) = k_{\parallel}(qh) \cos\theta \vec{x} + k_{\perp}(qh) \sin\theta \vec{y}. \quad (56)$$

Thus the differences between parallel and perpendicular susceptibilities ( $f$ 's and  $k$ 's) imply that the net current and force are generically not parallel to the applied field. Moreover, as the susceptibilities are of opposite sign, the net current (or the net force) is strictly perpendicular to  $\vec{E}_{\text{ext}}$  if the latter is applied at a specific angle  $\theta_j$  (or  $\theta_r$ ) with the  $x$  axis. From (55) and (56) these angles are given by

$$\begin{aligned} \tan^2(\theta_j) &= -f_{\parallel}(qh)/f_{\perp}(qh), \\ \tan^2(\theta_r) &= -k_{\parallel}(qh)/k_{\perp}(qh). \end{aligned} \quad (57)$$

This clearly provides a way to produce pumps sending flow in directions nonparallel to the applied field. Recall that  $\Phi$  may also be used as a tuning parameter, as it allows us to reverse the direction of current at fixed  $\vec{E}_{\text{ext}}$ .

A force is also generated on the upper plate at an angle with the applied field. However, this effect cannot be used to translate the upper plate (or to induce the steady rotation of a rotor), as the motion of the plate will modify  $\Phi$  and the electric geometry, and the effect averages out to zero as the  $+$ - symmetry is recovered. It is thus logical to inspect geometries that maintain symmetry breaking while allowing for the translation of the upper plate.

## V. NEUTRAL FLAT PLATE ON TOP OF AN UNDULATED CHARGE-MODULATED ONE

The simplest solution is of course to impose the charge modulation and the shape undulation on the same plate (for example the bottom one). The upper plate can be taken flat and uncharged, so that its motion does not affect the overall charge/shape geometry.

Furthermore, this solution is interesting on a ‘‘manufacturing’’ standpoint: the geometry of Sec. IV implies the ability to produce without defects periodic patterns on two plates of the same wavelength and to align them. The present geometry allows for defects as long as the chosen procedure grants that, e.g., positive (negative) charges are found in the valleys (hills) of the bottom plate. This could be achieved, for example, by depositing on a flat plate stripes of finite thickness of a material that tends to dissociate in contact with water (or adsorb specific charged groups). Eventually, in this geometry, the charge and shape effects will necessarily in-

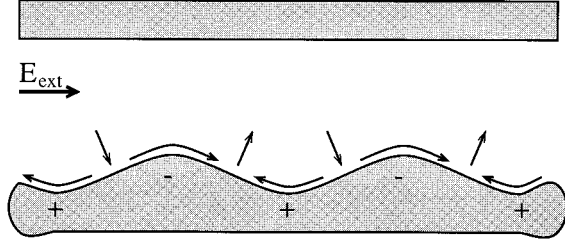


FIG. 4. A neutral flat plate on top of an undulated charge-modulated one. Parallel applied field. The recirculation pattern due to the charge modulation is bent by the undulation to produce a net flow toward the right. This effect is enhanced by the fact that the electric field is more intense in narrower regions, thus inducing a stronger electro-osmotic slip velocity (longer arrows). A homogeneous electro-osmotic flow results at infinity if the upper plate is absent.

teract even if the top plate is quite far away, as they take place in the same  $q^{-1}$ -thick layer of fluid above the bottom plate.

We follow the same steps as in Sec. IV to derive the fluid current and force on the upper plate generated by an applied electric field. To set notations, we consider an undulated and charge-modulated plate  $z^- = -h[1 + \alpha \cos(qx + \Phi)]$  and  $\zeta^- = \zeta_0 \cos(qx)$  below a flat neutral one  $z^+ = h$ . We solve at first order in  $\alpha$  the hydrodynamic problem defined by the boundary conditions  $\vec{v}(x, z^-) = \mu_0 \cos(qx) \vec{E}_{\text{ext}}^*(x, z^-)$  and  $\vec{v}(h) = \vec{0}$ .

#### A. $\vec{E}_{\text{ext}}$ parallel to charge modulation and undulation

We have to reevaluate the field  $\vec{E}_{\text{ext}}^*$  corresponding to an applied parallel field  $\vec{E}_{\text{ext}}^{\parallel} = E_{\parallel} \vec{x}$  (Fig. 4). Clearly, one still has  $E_{\text{ext}}^{*(0)} = E_{\text{ext}}^{\parallel}$ , but  $\vec{E}_{\text{ext}}^{*(1)}$  now derives from the potential

$$V^{*(1)}(x, z) = h E_{\parallel} \frac{\cosh[q(z-h)]}{\sinh(2qh)}. \quad (58)$$

Then as in Sec. IV A, the first-order analysis leads to a periodic stream function (period  $\pi/q$ ) plus a shear flow. Going through painful but straightforward algebra, the current and force on the top plate appear in the now familiar form

$$\vec{J}_{\parallel} = -\frac{\mu_0 h}{2} \vec{E}_{\text{ext}}^{\parallel} \alpha \cos(\Phi) F_{\parallel}(qh), \quad (59)$$

$$\vec{\tau}_{\parallel} = -\frac{\eta \mu_0 \vec{E}_{\text{ext}}^{\parallel}}{4h} \alpha \cos(\Phi) K_{\parallel}(qh), \quad (60)$$

where

$$F_{\parallel}(u) = K_{\parallel}(u) - 1, \quad (61)$$

$$K_{\parallel}(u) = -u \left[ \frac{u - \sinh(u) \cosh(u) \cosh(2u)}{\sinh^2(u) \cosh^2(u) - u^2} - \coth(2u) \right]. \quad (62)$$

Note that  $\vec{v}^{(0)}$  enters in a subtle manner into the calculation of  $\vec{J}_{\parallel}$  as the integration of  $v_x$  must be done from  $z^-$  (and not  $-h$ ) to  $z^+ = h$ .

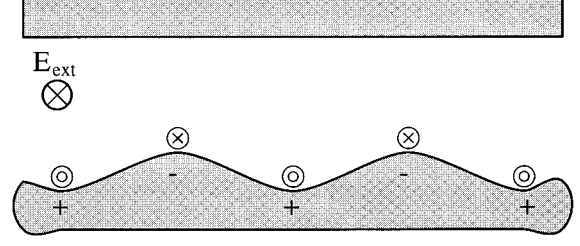


FIG. 5. A neutral flat plate on top of an undulated charge-modulated one. Perpendicular applied field. Although the force on the upper plate is always in the same direction as the field (for this choice of parameters), the direction of the average current depends on the separation between the plates. A homogeneous electro-osmotic flow along the field results at infinity if the upper plate is absent.

From an analysis of (62),  $K_{\parallel}$  and  $F_{\parallel}$  are both positive, with limiting behaviors  $F_{\parallel}(u \rightarrow 0) \approx \frac{3}{2}$ ,  $K_{\parallel}(u \rightarrow 0) \approx \frac{5}{2}$ , and  $F_{\parallel}(u \rightarrow \infty) = K_{\parallel}(u \rightarrow \infty) \approx 3u$ .

#### B. Perpendicular field $\vec{E}_{\text{ext}}^{\perp}$

If the electric field is applied perpendicular to the modulation  $\vec{E}_{\text{ext}}^{\perp} = E_{\perp} \vec{y}$  (Fig. 5), an analysis similar to Sec. IV B leads to

$$\vec{J}_{\perp} = -\frac{\mu_0 h}{2} \vec{E}_{\text{ext}}^{\perp} \alpha \cos(\Phi) F_{\perp}(qh), \quad (63)$$

$$\vec{\tau}_{\perp} = -\frac{\eta \mu_0 \vec{E}_{\text{ext}}^{\perp}}{4h} \alpha \cos(\Phi) K_{\perp}(qh), \quad (64)$$

where

$$F_{\perp}(u) = u \coth(2u) - 1 = K_{\perp}(u) - 1, \quad (65)$$

$$K_{\perp}(u) = u \coth(2u). \quad (66)$$

Now  $K_{\perp}$  is always positive with limits  $K_{\perp}(u \rightarrow 0) \approx \frac{1}{2}$  and  $K_{\perp}(u \rightarrow \infty) \approx u$ , whereas  $F_{\perp}$  changes sign, as shown by the limiting behaviors  $F_{\perp}(u \rightarrow 0) \approx -\frac{1}{2}$  and  $F_{\perp}(u \rightarrow \infty) \approx u$ .

#### C. Lubrication approximation $qh \ll 1$

To check the preceding results in the lubrication approximation, it is useful to use the top plate as the origin of the  $z$  axis, so that the charged bottom plate is given by  $z = -d(x)$ . Then a quick analysis shows that the formula (50)–(52) still hold. Applied to the geometries of Secs. V A and V B, they give back the  $qh \rightarrow 0$  limits of formulas (59)–(66).

#### D. Generic applied field and discussion

The analysis of subsection IV D can be repeated to obtain the effect of a field  $\vec{E}_{\text{ext}}$  applied at some angle  $\theta$  with the charge-modulation and undulation direction  $x$ . A general point is still valid: even for (on average) neutral plates, a net current and a net force on the upper plate are generated, with components transverse to the applied field. However, the susceptibilities calculated in the present section lead to significant qualitative differences.

(i) As to the generation of a net current flow, from (57) the latter can be purely perpendicular to the applied field only if  $F_{\perp}$  is negative (and thus of opposite sign that  $F_{\parallel}$ ). This requires a gap thin enough so that  $qh/\coth(2qh) < 1$ . If such is not the case, the generated current will still be generically at some angle with the applied field.

(ii) As to the force generated on the top plate, as  $K_{\parallel}$  and  $K_{\perp}$  are of the same sign, it is not possible to generate a force purely perpendicular to the applied field. However, as for the current, a component perpendicular to the applied field is generated. If the plate is held in the direction parallel to the field, it will thus slide perpendicularly to it. Similarly, a rotor would be set in helical motion, so that if its translation is prevented, it would simply rotate perpendicular to its axis. Note that a way to impede motion in the direction of the field is to add a slight *uniform* charge density (or order  $\alpha$  compared to the modulation amplitude) to create a simple electro-osmotic flow opposing the parallel component in the equivalent of (54).

(iii) Let me emphasize a structural difference from the geometry of Sec. IV. It can be seen from Eqs. (59)–(66) that even if the top plate is infinitely far from the bottom charge-modulated and undulated one, uniform flow is created in the region  $h \gg z_{\perp} \gg q^{-1}$ , due to the interaction of shape and charge in the region of thickness  $\approx q^{-1}$  above the bottom plate. This is clearly allowed as long as the  $+-$  symmetry is broken by the bottom plate alone. So if an external field  $\vec{E}_{\text{ext}} = E_{\parallel}\vec{x} + E_{\perp}\vec{y} = E_{\text{ext}}\vec{u}_{\theta}$  is applied, the velocity field above a single charge-modulated and undulated plate reaches a constant value

$$\vec{v}_{\infty} = -\frac{\mu_0 q h}{4} E_{\text{ext}} \alpha \cos(\Phi) (3 \cos \theta \vec{x} + \sin \theta \vec{y}). \quad (67)$$

This indicates that such a single plate immersed in a solution would tend to translate at some angle with an applied electric field, although the plate is on average neutral. This is very similar to the findings of Anderson [3] that the electrophoretic mobility of an object depends on the *charge distribution* on the object, and not solely on its *total charge*. An object of total positive charge can thus move as if it was uniformly negatively charged. Similarly, corrugated walls of *average positive charge* can induce an electro-osmotic flow in the direction of the field (as if they were *uniformly* negatively charged). Physically, charges that are in dips are hydrodynamically and electrostatically “screened” and thus less efficient to induce fluid motion. In our present geometry this screening is different for parallel and perpendicular applied fields (in the latter case there is actually no electrostatic screening), thus the angle between the flow (the force) and the applied field. The second plate is not necessary here, and a single object with the proper symmetry will be set into helical motion.

## VI. CONCLUSION

To summarize, we have investigated the consequence of charge nonuniformity on the generation of electro-osmotic flow and drag in a slab geometry. A modulation of the charge density on the wall induces convective patterns that can be taken advantage of to generate fluid currents and drag

on the plates, provided one breaks the  $+-$  symmetry, e.g., by modulating the shape of the plates. This could be of use in microfabricated geometry to design pumps or motors.

Note that we have neglected what might be a simpler design, namely uniform charge densities and only shape modulation. Consider, e.g., a slab geometry with the bottom plate undulated and uniformly charged. It is easy to show that the electro-osmotic flow generated parallel and perpendicular to the undulation are of different amplitudes, so that transverse components can also be generated. However, this effect is only of order 2 in the amplitude of the undulation  $\alpha$  (on symmetry grounds it has to be an even power), whereas the component parallel to the applied field is of zeroth order. The difference from the situation of Secs. IV and V is clear. Here the field pushes the fluid rather homogeneously, and is simply slightly less efficient in doing so in one direction. In Secs. IV and V the field creates an almost periodic and symmetric pattern of pushing and pulling which is exploited by the undulation, allowing an efficient transfer in the transverse direction. However, in situations where large amplitude undulations are possible, uniformly charged undulated walls can be efficient generators of transverse effects. Eventually, as mentioned in Sec. V D, uniform and modulated charge densities can be combined to induce specific geometric features.

Another important remark is that we have focused on periodic geometries with uniform applied currents, and thus completely neglected boundary and finite-size effects. These may break the  $+-$  symmetry even for flat walls. In finite-size systems where only a few stripes are present, it is thus legitimate to consider additional geometries, e.g., undulation and charge modulations along different axes, whereas these are ruled out on symmetry grounds for infinite systems. This is also clearly of importance to discuss the design of finite-size mobile parts: e.g., for a rotor the radius and the length of the cylinder (compared to the stripe size), as well as the phase of the modulation, have to be taken into account [11].

Finally, the present analysis seemingly does not take into account the polarization charges that will appear generically on the wall surfaces. Let me here show that, at first order in  $\vec{E}_{\text{ext}}$ , and for the thin Debye layers (TDL's) considered in Secs. IV and V, this should not modify the results obtained for the fluid current in the slab  $\vec{J}$  and the average force density on the upper plate  $\vec{\tau}$ .

*Polarization charges.* The walls have up to now been taken to be almost perfectly insulating compared to the electrolyte of high conductivity. As a result electric field lines have been assumed parallel to the interfaces. The continuity of the tangential component of the electric field will then impose inside the walls a nonvanishing normal component of the electric displacement. The corresponding discontinuity leads to polarization charges of density  $\sigma_{\text{pol}}$  proportional to the dielectric constant of the wall  $\epsilon_{\text{wall}}$ . Note first that these charges do not exist in a purely flat geometry, and are thus proportional to  $\alpha$  at first order. More importantly, they are proportional to the applied field  $E_{\text{ext}}$ .

*Corrections induced.* The corresponding modification of the ionic density  $\rho_e$  in the fluid is thus also linear in  $E_{\text{ext}}$ . Therefore it can produce a flow at the same order through the last term on the right-hand side of Eq. (1) only by coupling

to the *equilibrium* electric field. The latter being almost perpendicular to the interface in the TDL approximation, this results only in a pressure term that can be absorbed in the definition of  $p$  [a similar result has already been made explicit for low electrostatic surface potentials in Eq. (3)]. Approximations (4)–(6) thus remain valid, and the flow induced at first order in  $E_{\text{ext}}$  is independent of the polarization of the walls. Consequently, this also holds for the hydrodynamic forces on the upper plate. At this order, there are furthermore no electrical forces on the upper plate, as the equilibrium field is zero in their vicinity so that polarization charges can induce only a term proportional to  $E_{\text{ext}}^2$ . Thus our results for  $\vec{J}$  and  $\vec{\tau}$  correctly describe the linear response to the applied field  $\vec{E}_{\text{ext}}$ , at least as long as the finite-size effects mentioned in the previous paragraph are negligible.

In conclusion, the combination of charge and shape effects seems a promising way to generate a wide variety of electromechanical effects, where three-dimensional flows arise with the symmetries and characteristics imposed by surface-drawn patterns.

#### ACKNOWLEDGMENTS

This study emerged from discussions with Jacques Prost. Nigel Cooper and Howard A. Stone contributed through many useful comments. I benefited from the partial support of NSF Grants Nos. DMR91-06237, DMR94-17047, and DMR94-16910 to realize this work, and from the kind hospitality and nice atmosphere of the Center for Studies in Physics and Biology (Rockefeller University), to finish it.

- 
- [1] W. B. Russel, D. A. Saville, and W. R. Schowalter, *Colloidal Dispersions* (Cambridge University Press, Cambridge, 1989).  
 [2] D. A. Saville, *Annu. Rev. Fluid Mech.* **9**, 321 (1977).  
 [3] J. L. Anderson, *Annu. Rev. Fluid Mech.* **21**, 61 (1989).  
 [4] P. D. Grossman and J. C. Colburn, *Capillary Electrophoresis, Theory and Practice* (Academic, San Diego, 1992).  
 [5] P. E. Lammert, R. Bruinsma, and J. Prost, *J. Theor. Bio.* (to be published).  
 [6] J. L. Anderson, *J. Colloid Interf. Sci.* **105**, 45 (1985); M. C. Fair and J. L. Anderson, *ibid.* **127**, 388 (1989).  
 [7] J. R. Melcher and G. I. Taylor, *Annu. Rev. Fluid Mech.* **1**, 111 (1969), and references therein.  
 [8] R. M. Berry, *Biophys. J.* **64**, 961 (1993).  
 [9] J. Prost (private communication).  
 [10] A. Ajdari, *Phys. Rev. Lett.* **75**, 755 (1995).  
 [11] J. Prost and F. Gerbal (unpublished).